# Bypassing Eutectics with Extractive Crystallization: Design Alternatives and Tradeoffs

**Susan R. Dye and Ka M. Ng**
Dept. of Chemical Engineering, University of Massachusetts, Amherst, MA 01003

*A systematic design method reported here uses extractive crystallization to separate a three-component mixture despite the presence of eutectics. Phase behavior can be classified into six basic types, and six flowsheet structures can handle systems with any of these solid-liquid-phase behaviors. Design equations are formulated for these flowsheet structures, and design variables and constraints are identified. In addition, design issues, such as the choice of solvent, the effect of design variables on recycle flows, and the magnitude of the costs, are discussed.*

## Introduction

Distillation has been the workhorse in the chemical industry primarily because it allows the complete separation of a multicomponent mixture of chemicals into pure components; however, it is not cost-effective for close-boilers such as para- and metaxylene. Furthermore, it is not suitable for many biochemicals, monomers, polymers, and inorganics that either have high boiling points or are heat-sensitive. For these materials, crystallization is generally the technique to use because, like distillation, it produces a high-purity product (Paul and Rosas, 1990). With the gradual shift of emphasis from commodity to specialty chemicals in the chemical industry, crystallization is expected to play an increasingly significant role in separations.

The singular problem in the complete separation of a mixture by means of crystallization is caused by the presence of eutectics, where two or more components cocrystallize. The common practice in the processing industry is to recover a single, pure component up to the eutectic composition (Barnicki and Fair, 1990). This, of course, does not solve the entire separations problem. The mother liquor in the effluent of the crystallizer may still contain a substantial amount of the desired component, necessitating a large recycle or purge stream. Also, this approach is obviously not appropriate when the recovery of two or more components is desired.

Extractive crystallization offers complete separation by bypassing the eutectics with the introduction of an additional component to the system. The early development of extractive crystallization was described by Findlay and Weedman (1958). The focus was on the separation of meta- and paraxylene by the addition of a hydrocarbon solvent such as *n*-pentane and *n*-heptane. The same technique was used to separate meta- and paracresol, and ortho- and paranitrochlorobenzene (Chivate and Shah, 1956; Dikshit and Chivate, 1970; Tare and Chivate, 1976), and benzene and cyclohexane (Nagahama et al., 1991). In an overview of extractive crystallization, Dale (1981) described various commercialized extractive crystallization processes, which include dewaxing of lube oil and separation of sterols.

The literature describes an extractive crystallization process that is system-specific and does not make clear how to generalize the synthesis of this process to separate any given binary mixture. Only recently has a systematic design procedure become available (Rajagopal et al., 1991). All possible phase diagrams are classified into two types—types I and II—depending on the relative locations of the feed composition and of the eutectic compositions on the ternary phase diagram. This general methodology can be used for the complete separation of two components, offering two equipment configurations, one for each of the two types of phase behavior. The procedure is applicable to systems with simple eutectics as well as systems with multiple eutectics and compound formation.

Since it is common for more than one separation technique to be used to separate a multicomponent mixture, the current methodology for binary mixtures is applicable to a considerable number of separations. For instance, in the xylene process described by Findlay and Weedman (1958), one can first remove ethylbenzene and orthoxylene from the feed stream using distillation before using extractive crystallization to separate the remaining binary mixture of para- and

Correspondence concerning this article should be addressed to K. M. Ng.

metaxylene. This argument, however, does not justify the absence of a more comprehensive extractive crystallization method that can separate more than two components. In process synthesis (Westerberg, 1987; Douglas, 1988; Rajagopal et al., 1992), it is highly desirable to have at one's disposal a comprehensive repertoire of separation techniques for generating process alternatives. For example, one recent question raised is whether or not it is possible to separate ethylbenzene, para-, and metaxylene using crystallization, extractive or otherwise (Douglas et al., 1993). Another example concerns the manufacture of adipic acid, an intermediate for nylon, where glutaric and succinic acids are also formed as by-products. A considerable amount of adipic acid can be lost in a liquid purge stream along with the by-products (Sciance and Scott, 1967). Given the 0.68 billion kg/yr production of adipic acid in the United States alone, a new crystallization process could have a significant economic impact.

Thus, the objective of this work is to formulate a systematic design method for using extractive crystallization to separate a three-component mixture, despite the presence of eutectics. Three-solute extractive crystallization provides the design engineer with an additional option in process synthesis. To facilitate the engineer's decision-making process, this article identifies the design variables and reports the sensitivity of the process to these variables. In addition, there is a discussion of various design issues such as solvent selection, effect of design variables on recycle flows, and costs.

## Phase Behavior

To understand the design procedure, it is necessary to examine the isobaric phase behavior of a simple-eutectic, four-component system depicted on a three-dimensional tetrahedron (Figure 1) (Ricci, 1951; Haase and Schönert, 1969). A point on or within the tetrahedron indicates the composition of a four-component liquid mixture that is saturated with respect to one or more of the four substances. Thus, although temperatures are not shown explicitly in Figure 1, associated with each point is the freezing temperature for the mixture. The apices indicate a pure substance, *A*, *B*, *C*, or *S*. A point on one of the six edges depicts a binary mixture. Any point on one of the four triangular faces of the tetrahedron is the composition of a liquid containing only three of the substances, the three that appear at the corners of the face. A liquid made up to *A*, *B*, *C*, and *S* has a composition represented by an interior point. The solutes to be separated are *A*, *B*, and *C*, and the substance that facilitates the separation is the solvent *S*.

There are six *binary eutectic points*, *AB*, *AC*, *AS*, *BC*, *BS*, and *CS*, one on each of the six edges. Also, there are four

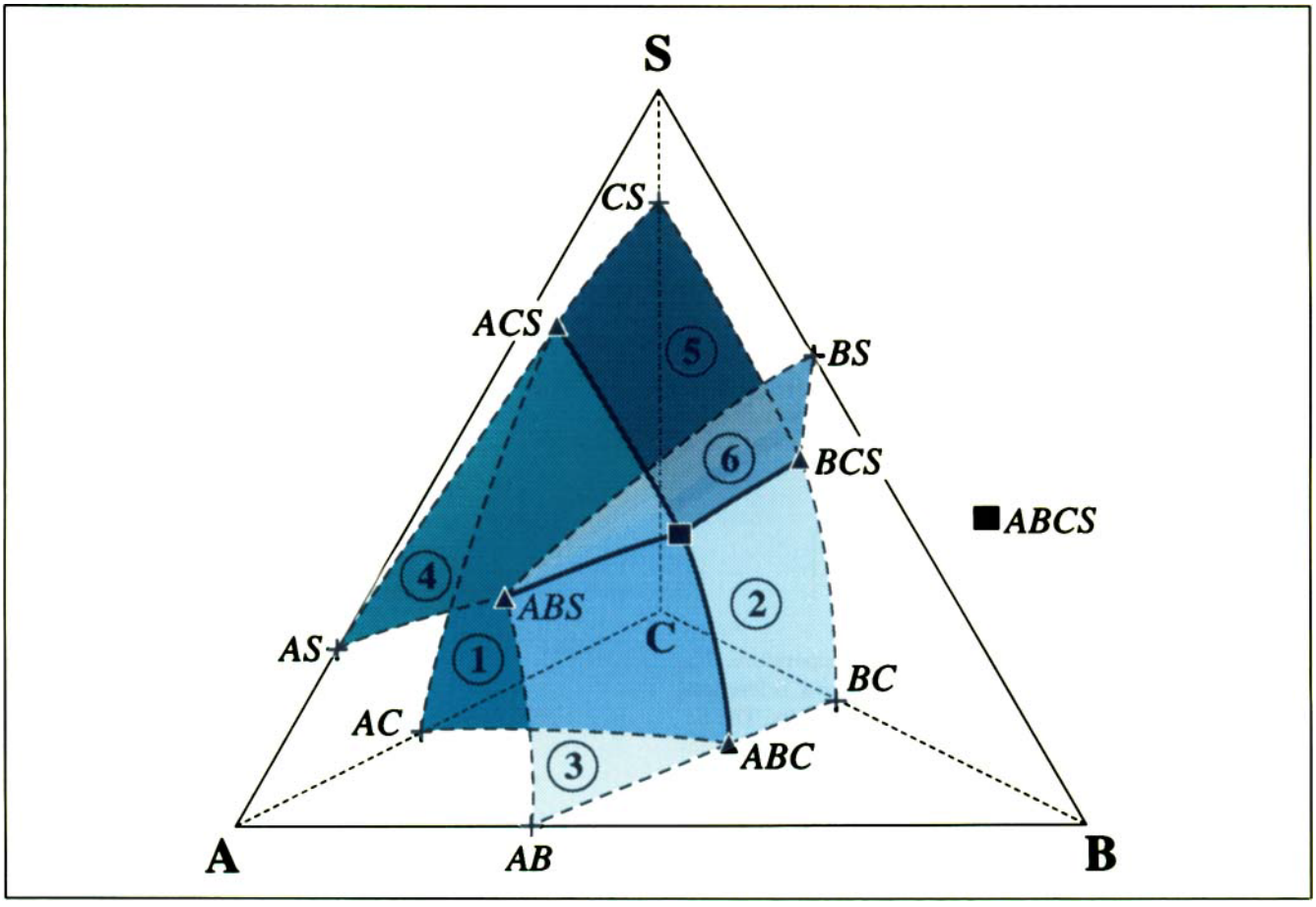


**Figure 1. Simple-eutectic, solid-liquid tetrahedral phase diagram for a quaternary system.**

*Key*: This key applies to all figures in this article, except Figure 16. ■ Quaternary eutectic; ▲ ternary eutectic; + binary eutectic; – – – double saturation trough; —— triple saturation trough.

*ternary eutectic points*, *ABC*, *ACS*, *ABS*, and *BCS*, one on each of the four triangular faces, and one *quaternary eutectic*, *ABCS*, in the interior. These eutectics are the points where two, three, or four components cocrystallize, respectively.

Six internal *double-saturation surfaces*, which are numbered in Figure 1, divide the tetrahedron into four *compartments*, each corresponding to a pure component. Surfaces 1, 3 and 4 form the boundaries of compartment *A*. Similarly, surfaces 2, 3 and 6 form the boundary of compartment *B*, and surfaces 1, 2 and 5, the boundary of compartment *C*. The double-saturation surfaces are the loci of liquid compositions for which two components precipitate out when crystallization takes place. For example, cocrystallization of *A* and *B* occurs on surface 3. The binary eutectic compositions are connected to the corresponding ternary eutectic compositions by *double-saturation troughs* (dashed lines), along which two components cocrystallize. At compositions along the four internal *triple-saturation troughs* (solid lines) connected to the quaternary eutectic, three solutes precipitate out during crystallization. For example, cocrystallization of *A*, *B*, and *C* occurs along the triple-saturation trough connecting *ABC* and *ABCS*. At the quaternary eutectic point, all four components precipitate out.

A liquid whose composition is represented by a point in compartment *A* can be cooled to form crystals that contain only *A*. The same effect, the production of a pure crystal, occurs in compartments *B* and *C*, as well. Thus, in an extractive crystallization separation, the location of the process streams is an important factor. As mentioned before, pure crystals do not form from a liquid whose composition is found on one of the internal surfaces. Consequently, the internal surfaces limit the crystallization of a pure component.

There are many possible phase behaviors. At present, a reliable theory for the prediction of behaviors such as compound formation or multiple eutectics does not exist. Some systems, particularly those made up of metals, form solid solutions, and the purification of such systems is not considered in this article (Gilbert, 1991; Slaughter and Doherty, 1995). On the other hand, organics commonly form simple-eutectic systems (Matsuoka, 1977). The calculation of the tetrahedral phase diagram for a simple-eutectic system begins with the following equation, which gives the maximum mole fraction of component *i* that can be maintained in solution at a temperature, *T* (Walas, 1985):

$$\gamma_i x_i = \gamma_i^s x_i^s \exp\left[\frac{\Delta H_{mi}}{R}\left(\frac{1}{T_{mi}} - \frac{1}{T}\right)\right]. \qquad (1)$$

The heat of fusion, $\Delta H_{mi}$, and the melting temperature, $T_{mi}$, are tabulated for many substances in standard references, such as the *CRC Handbook of Chemistry and Physics*. The liquid-phase activity coefficient, $\gamma_i$, can be predicted using any of the various excess Gibbs free-energy models. For a pure solid component or a eutectic mixture made up of immiscible pure solid components, the product of the activity coefficient and the mole fraction for the solid, $\gamma_i^s x_i^s$, is one.

An example of the use of Eq. 1 is the calculation of the quaternary eutectic composition, a composition at which four solids are in equilibrium with respect to a solution. This condition occurs at a temperature at which the mole fractions of the four components sum to unity:

$$1 = \sum_{i=A,B,C,S} \frac{1}{\gamma_i} \exp\left[\frac{\Delta H_{mi}}{R}\left(\frac{1}{T_{mi}} - \frac{1}{T}\right)\right]. \qquad (2)$$

Another example is that of the calculation of the compositions that make up a triple-saturation trough, where three solid phases are in equilibrium with a liquid containing four components. To locate such a trough, for example, the one connecting the ternary eutectic *ABC* and the quaternary eutectic *ABCS*, the solvent mole fraction is set to a value near zero. The following equation determines the temperature at which 1 minus the solvent mole fraction is equal to the sum of the mole fractions of the other three components:

$$1 - x_S = \sum_{i=A,B,C} \frac{1}{\gamma_i} \exp\left[\frac{\Delta H_{mi}}{R}\left(\frac{1}{T_{mi}} - \frac{1}{T}\right)\right]. \qquad (3)$$

The entire triple-saturation trough can be mapped out by gradually increasing $x_S$ until it reaches its value at the quaternary eutectic. Similar arguments can be used to obtain the other three triple-saturation troughs, the four double-saturation surfaces, and all of the binary and ternary eutectic points.

It is not easy to represent composition changes on a three-dimensional tetrahedral phase diagram, and a Jänecke projection provides a convenient alternative. Essentially, the Jänecke projection is the tetrahedral phase diagram compressed onto the base of the tetrahedron as viewed from the apex *S*. Figure 2 is the Jänecke projection of the phase diagram of Figure 1, where the double-saturation troughs (dashed lines) and the triple-saturation troughs (solid lines) outline compartments *A*, *B* and *C*. There are two features that can be used to distinguish Jänecke phase diagrams from one another. The first feature involves the orientation of each surface. Since the projection of the solid line *ACS-ABCS* appears closer to *A* than the dashed line *AC-ABC*, surface 1 is

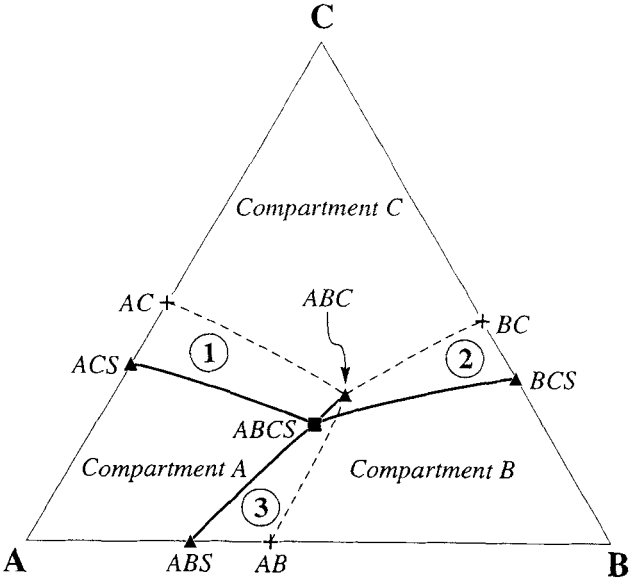


**Figure 2. Jänecke projection of the tetrahedral phase diagram.**

**Table 1. Six Basic Phase Diagrams for a Quaternary System**

| Type | Phase Diagram Characteristics: Proj. Location of Quat. Eutectic | Phase Diagram Characteristics: Orientation of Relevant Surface | Process Config. for Sep. |
|---|---|---|---|
| PD1 | Compartment *B* | Surface 1; leans toward *C* | Ia and IIIa |
| PD2 | Compartment *B* | Surface 1; leans toward *A* | IIa and IIIa |
| PD3 | Compartment *A* | Surface 2; leans toward *B* | IIa and IIIa |
| PD4 | Compartment *A* | Surface 2; leans toward *C* | IIb and IIIb |
| PD5 | Compartment *C* | Surface 3; leans toward *A* | Ib and IIIb |
| PD6 | Compartment *C* | Surface 3; leans toward *B* | Ib and IIIb |

said to *lean toward A* with respect to *S*. On the other hand, surface 3 *leans away from B* with respect to *S*. The second distinguishing characteristic of Jänecke phase diagrams is the projected location of the quaternary eutectic. In Figure 2, the projected location of the quaternary eutectic is in compartment *A*.

The phase behavior of three-solute systems can be classified into six types, designated as PD1 through PD6 (phase diagram 1 through 6), based on the two distinguishing features of Jänecke phase diagrams. This classification is made with the understanding that the projected location of the feed composition is assumed to be in compartment *A*. These six types are listed in Table 1 along with the two important characteristics of each phase diagram. Also given in Table 1 are the specific process configurations that would apply to each of the six phase diagrams. These separations are discussed below.

## General Methodology

The objective of an extractive crystallization separation is to precipitate out a pure solute from a stream with a composition that lies in one of the solute compartments of the phase diagram. In an actual separation, there would be at least one process composition in each of the three compartments *A*, *B*, and *C* so that each substance could be crystallized in pure form. After one component is crystallized and filtered from the process, the next step is to cross an internal surface to a new compartment and crystallize another component. Presented below are the three operations that can effect such a crossing, that is, alteration of the composition of a stream such that the new composition is in another compartment.

The first operation is pictured in Figure 3. Stream 1, which has a composition 1 in compartment *A*, is combined with stream 3, whose composition is represented by point 3 in compartment *B*. The result is composition 2, which is in compartment *B*. This operation is referred to as *stream combination*. The second operation that moves the composition to a new compartment is *solvent removal*. In Figure 4, composition 1 is located in compartment *C*. Upon the removal of solvent, composition 1 moves away from the apex denoted by *S*. In doing so, it crosses surface 2 and enters compartment *B*. This operation is generally accomplished with an evaporator or a distillation column. The third operation, simply the reverse of the second, is *solvent addition*. In Figure 4, a solvent would be added to composition 2 to give composition 1. The process path moves toward point *S* and into compartment *C*. This operation is a special case of stream combination in which one of the two combined streams consists entirely of the solvent.

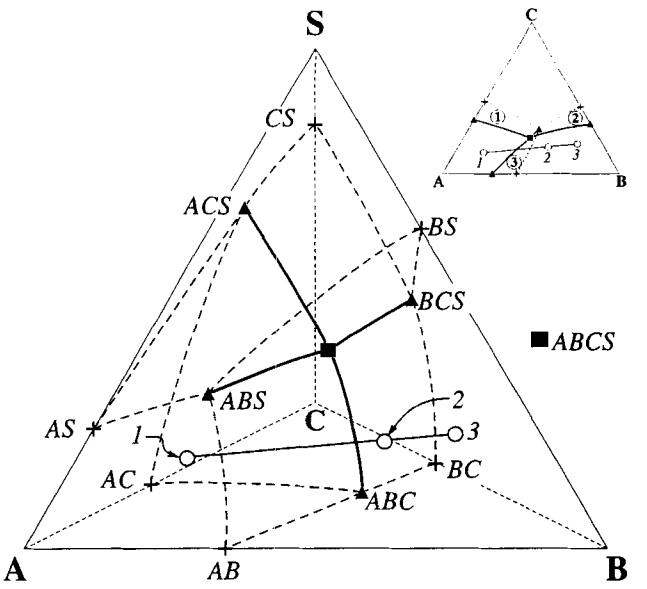


**Figure 3. Composition changes brought about by stream combination.**

*Key*: This key applies to Figures 3–15, 17, and 18. ○ Composition that is located within the interior of the tetrahedron; —— tie lie.

The double-saturation surfaces that form the compartments present barriers that must be crossed so that all three solutes can be recovered in pure form. In the separation of a ternary system, there are three crystallizers and two double-saturation surfaces to cross. For example, if the feed of *A*, *B*

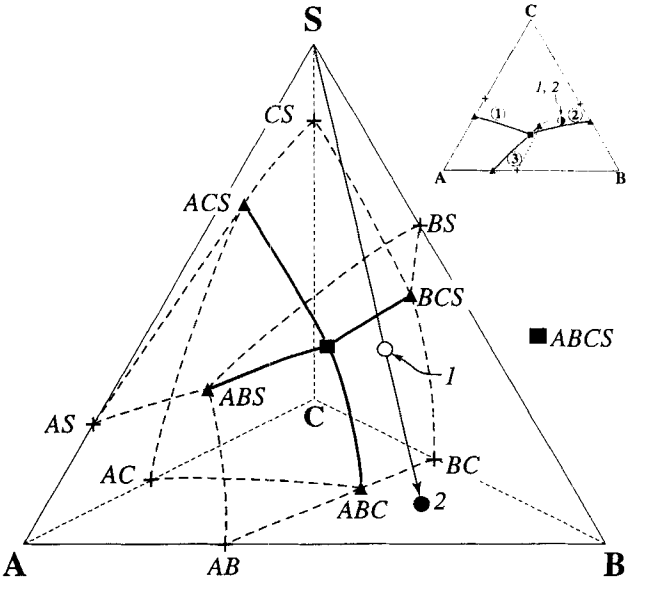


**Figure 4. Composition changes brought about by solvent removal or addition.**

*Key*: This key applies to Figures 4–15, 17, and 18. ● Composition that lies on the *ABC* base of the tetrahedron; ○ composition that is located within the interior of the tetrahedron; ◐ first composition lies on the *ABC* base of the tetrahedron, and the second, in the interior; ◑ first composition is located in the interior of the tetrahedron, and the second, on the base.

and $C$ were to lie in compartment $A$ of Figure 1 and if the separation were to be carried out clockwise, the first crystallizer would crystallize pure $A$. In order for pure $C$ to be solidified in the second crystallizer, surface 1 must be crossed between the first and second crystallizer. Similarly, surface 2, which is shared by compartments $C$ and $B$, must be crossed between the second and third crystallizers.

Since there are three operations and two surfaces to cross, one would expect that there are $3^2$, or 9, separation schemes. However, stream combination has been eliminated as a possible operation to use after the second crystallizer because the recycle should not be directed back into the third crystallizer. This point will become clear when we examine the flowsheet configurations. Thus, the flowsheets can be organized into six ($3\times2$) combinations as shown in Table 2. Discussed below are the six process configurations: types Ia, Ib, IIa, IIb, IIIa, and IIIb. The Roman numerals indicate the operation used between the first and second crystallizers, and the letters specify the operation used between the second and third crystallizers. Roman numeral I represents solvent removal, II represents solvent addition, and III represents stream combination. Similarly, the letter "a" stands for solvent removal, and "b" for solvent addition. The process compositions for each three-solute separation are also plotted on a Jänecke projection as they are viewed from the point $S$. The composition numbers on the phase diagrams correspond to the stream numbers of the flowsheets. It should be noted that some features of the phase diagrams are exaggerated in order to allow the composition changes to be marked clearly.

**Table 2. Six Process Configurations for the Separation of a Three-Solute System**

| Type | Location/Technique: Between Crystall. 1 and 2 | Between Crystall. 2 and 3 | At Feed or After Crystallizer 3 |
|---|---|---|---|
| Ia | Solvent removal | Solvent removal | Solvent addition and stream combination |
| Ib | Solvent removal | Solvent addition | Stream combination |
| IIa | Solvent addition | Solvent removal | Stream combination |
| IIb | Solvent addition | Solvent addition | Solvent removal and stream combination |
| IIIa | Stream combination | Solvent removal | Solvent addition |
| IIIb | Stream combination | Solvent addition | Solvent removal |

### *Type Ia flowsheet configuration*

Let us begin with the arrangement of equipment for the type Ia separation (Figure 5a). Type Ia separation differs from the other five in that it employs two evaporators, rather than one. As shown in Table 1, type Ia is best suited for the separation of three solutes that exhibit PD1 phase behavior, for which the identifying features are that the projection of the quaternary eutectic is in compartment $B$ and that surface 1 leans toward $C$. Figure 5b is a Jänecke projection of the phase diagram and of the type Ia process compositions. Figure 5c is a three-dimensional representation of the same separation.

Figures 5a, 5b, and 5c indicate that the initial step is the mixing of the solute recycle, stream 7, and the feed, stream $F$. Stream 1 has a composition that lies on a tie-line between streams 7 and $F$. Since these streams do not contain solvent, they lie on the $ABC$ triangular base of the phase diagram and their compositions are represented by blackened circles.

In the next step, the solutes in stream 1 are mixed with the solvent of stream 10, resulting in stream 2. Both compositions 1 and 2 are represented by the same circle on the phase diagram of Figure 5b because, from the point of view of the solvent, composition 2 would not appear in a location different from that of composition 1; however, the circle is only half-blackened because composition 1 is located on the base of the phase diagram and composition 2 is not. Stream 2 is directed to the first crystallizer and filter; the composition moves on a straight line away from compositions $A$ and 2 so that 3 is the new composition. Composition 3 is located above the $ABC$ base of the tetrahedral phase diagram and above surface 1. Surface 1 is crossed between streams 3 and 4 by solvent removal, which is possible because the surface leans toward $C$. Since streams 3 and 4 both contain solvent, their compositions are represented by open circles.

Composition 4 is located in compartment $C$, and therefore it is possible to remove pure $C$ from this stream, creating stream 5. Since surface 2 leans toward $B$, solvent removal is an appropriate choice of operation to apply to stream 5. This second solvent removal is complete, separating the remaining solvent from the solutes and moving the process composition into compartment $B$. This results in composition 6, which is in compartment $B$, and a quantity of $B$ can be recovered in the third crystallizer. The solutes that are not crystallized leave the third crystallizer in stream 7 and are combined with the feed, thus continuing the separation cycle.

For the type Ia separation described earlier to be possible, the feed composition must be located in compartment $A$. Furthermore, the feed composition must be on the left side of an imaginary line that connects $A$ with the quaternary eutectic, $ABCS$. This condition applies to all six separation types. If the condition is not met, a counterclockwise separation should be considered: first $A$ is removed, after which $B$ then $C$ are removed.

### *Design equations for type Ia*

Material balances establish the compositions and flow rates of all the streams in the process. To begin, examine the balances for the recycle of the solutes in Figure 5a. Since stream 10 consists of pure solvent and since only $A$ is recovered in the first crystallizer, the total amount of $B$ in stream 3 is the sum of the feed of $B$, $F_{BF}$, and the recycle of $B$, $F_B(7)$. The total flow rate of stream 3 is $[F_{BF} + F_B(7)]/x_B(3)$. The amount of $A$ in the feed is completely removed in the first crystallizer and filter. Therefore, the recycle of $A$ must be that portion of the total flow rate of stream 3 that is made up of $A$:

$$F_A(7) = \frac{F_{BF} + F_B(7)}{x_B(3)} x_A(3). \tag{4}$$

Similarly, the recycle of the components $B$ and $C$ are

$$F_B(7) = \frac{F_A(7)}{x_A(7)} x_B(7) \tag{5}$$

$$F_C(7) = \frac{F_A(7)}{x_A(7)} x_C(7). \tag{6}$$

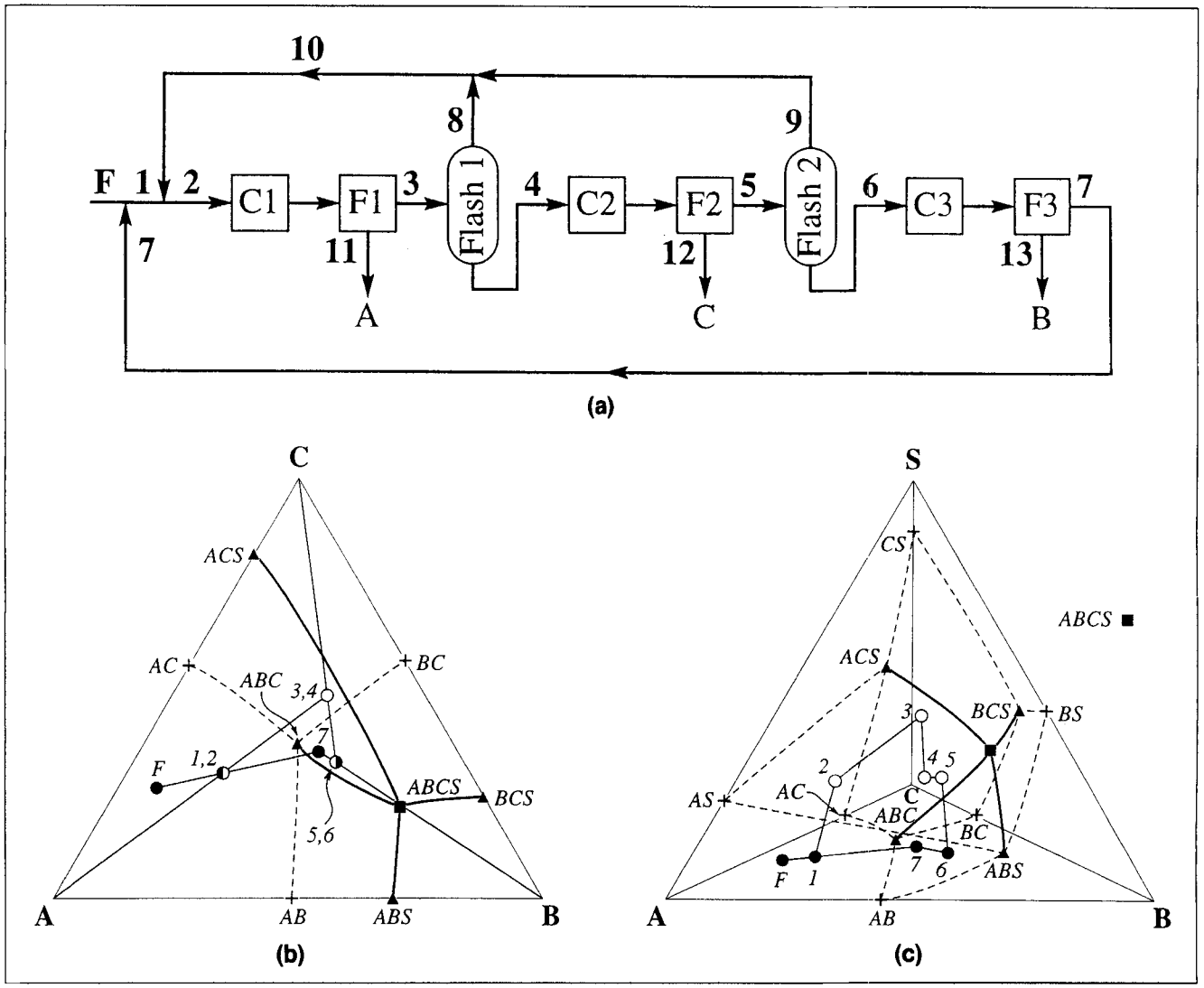


**Figure 5. (a) Type Ia process flowsheet; (b) type Ia process flowsheet applied to the separation of a system showing PD1 solid-liquid phase behavior; (c) type Ia process paths as they appear on a tetrahedral phase diagram.**

Substitution of Eq. 5 into Eq. 4 gives

$$F_A(7) = \frac{F_{BF}}{\dfrac{x_B(3)}{x_A(3)} - \dfrac{x_B(7)}{x_A(7)}}. \tag{7}$$

Thus, the recycle balances for $B$ and $C$ are

$$F_B(7) = \left[\frac{F_{BF}}{\dfrac{x_B(3)}{x_A(3)} - \dfrac{x_B(7)}{x_A(7)}}\right]\frac{x_B(7)}{x_A(7)} \tag{8}$$

$$F_C(7) = \left[\frac{F_{BF}}{\dfrac{x_B(3)}{x_A(3)} - \dfrac{x_B(7)}{x_A(7)}}\right]\frac{x_C(7)}{x_A(7)}. \tag{9}$$

The two solvent recycle streams, 8 and 9, together form stream 10. The flow rates of these three streams are given by the following material balances:

$$F_S(9) = [F_{BF} + F_B(7)]\frac{x_S(5)}{x_B(5)} \tag{10}$$

$$F_S(8) = [F_{BF} + F_B(7)]\frac{x_S(3)}{x_B(3)} - F_S(9) \tag{11}$$

$$F_S(10) = [F_{SF} + F_B(7)]\frac{x_S(3)}{x_B(3)}. \tag{12}$$

Most of the stream compositions and flow rates are dependent variables and are fixed by the material balances. However, four design variables must be chosen so that the

specification of the process is complete. The following have been selected:

$x_S(3)$ = mole fraction of solvent in stream 3

$x_S(5)$ = mole fraction of solvent in stream 5

$x_B(3)/x_A(3)$ = ratio of the mole fraction of $B$ to the mole fraction of $A$ in stream 3

$\boldsymbol{x}(7)$ = mole fractions for stream 7

The four design variables just listed are limited by several factors. First, that no flow rate can be negative means

$$\frac{x_B(3)}{x_A(3)} > \frac{x_B(7)}{x_A(7)}. \tag{13}$$

This restricts the values of $\boldsymbol{x}(7)$ and $x_B(3)/x_A(3)$. Other constraints are due to the geometric requirements that the compositions of streams 1 through 7 must be located in their appropriate, respective compartments, as indicated by Figures 5b and 5c. We will return to this point at a later stage.

### *Other separation types*

Discussed below are the other five flowsheets, applied to

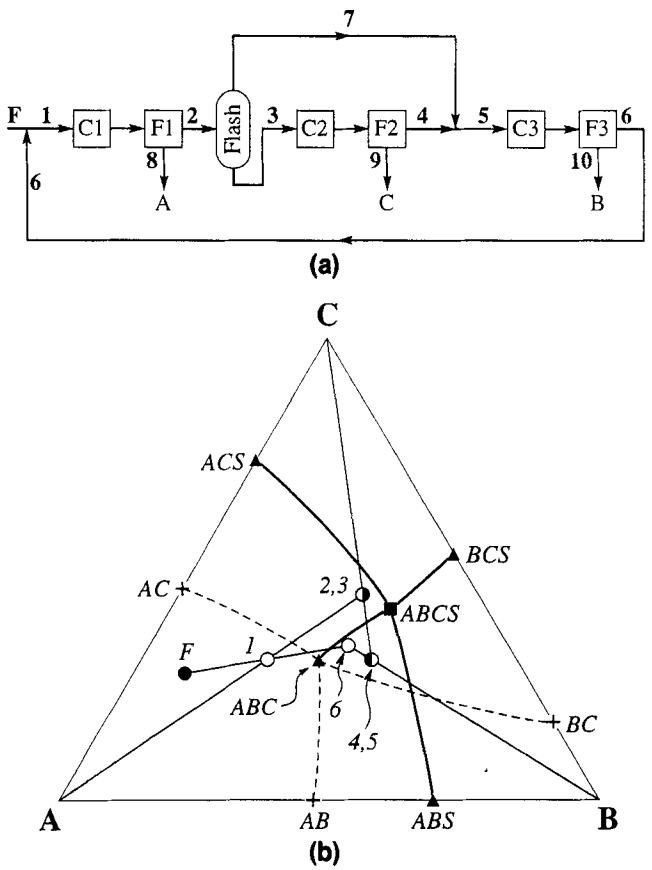


**Figure 6. (*a*) Type Ib process flowsheet, (*b*) type Ib process flowsheet applied to the separation of a system showing PD6 solid-liquid phase behavior.**

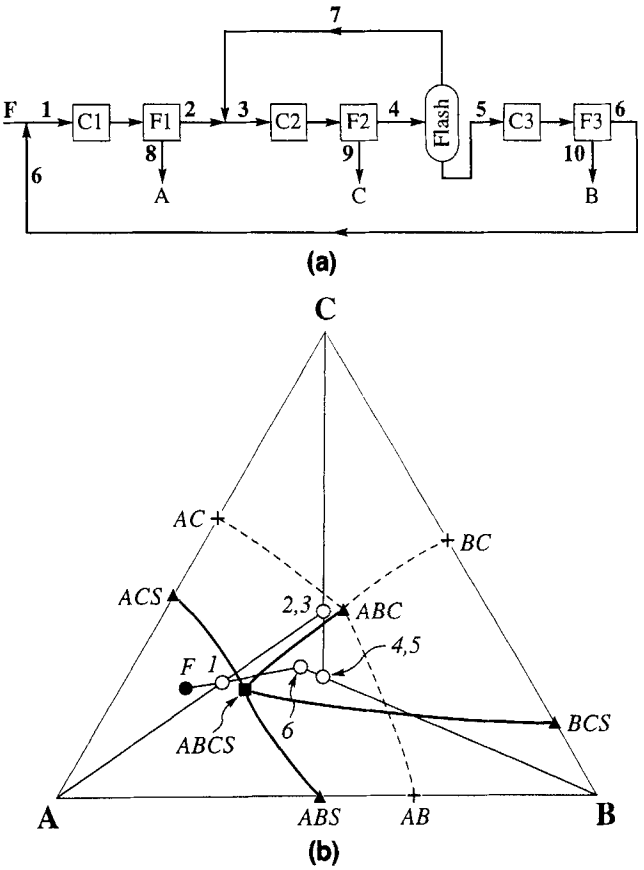


**Figure 7. (*a*) Type IIa process flowsheet; (*b*) type IIa process flowsheet applied to the separation of a system showing PD3 solid-liquid phase behavior.**

PD1, PD3, PD4, and PD6. Because of space limitations, detailed discussions of PD2 and PD5 are reported elsewhere (Dye, 1995). For type Ib, solvent removal is used between the first two crystallizers, as is done in type Ia. Solvent addition, however, is the operation used between the second and third crystallizers (Figure 6a). Figure 6b is a PD6 projected phase diagram with the type 1b process compositions. The first step of the separation is the recycling of solutes back to the feed stream. Next, stream 1 is fed to the first crystallizer, where the removal of an amount of $A$ equal to that in the feed gives composition 2. Surface 1 leans away from $A$, and therefore solvent removal positions composition 3 in compartment $C$. When $C$ is removed, the resulting composition should be positioned in the triangular region where surface 3 overlaps 2. Thus, since surface 2 leans toward $C$, solvent addition enables composition 5 to be located in compartment $B$. The amount of additional solvent should place composition 5 between surfaces 2 and 3; too much solvent would put composition 5 above surface 3 and in compartment $A$. As long as composition 5 is positioned correctly in compartment $B$, pure $B$ can be recovered in the third crystallizer.

The equipment arrangement for the type IIa separation is shown in Figure 7a. Figure 7b is a Jänecke projection of the PD3 phase diagram and of the type IIa process compositions. Type IIa separation is essentially the reverse of Ib; first solvent addition is used and then solvent removal.

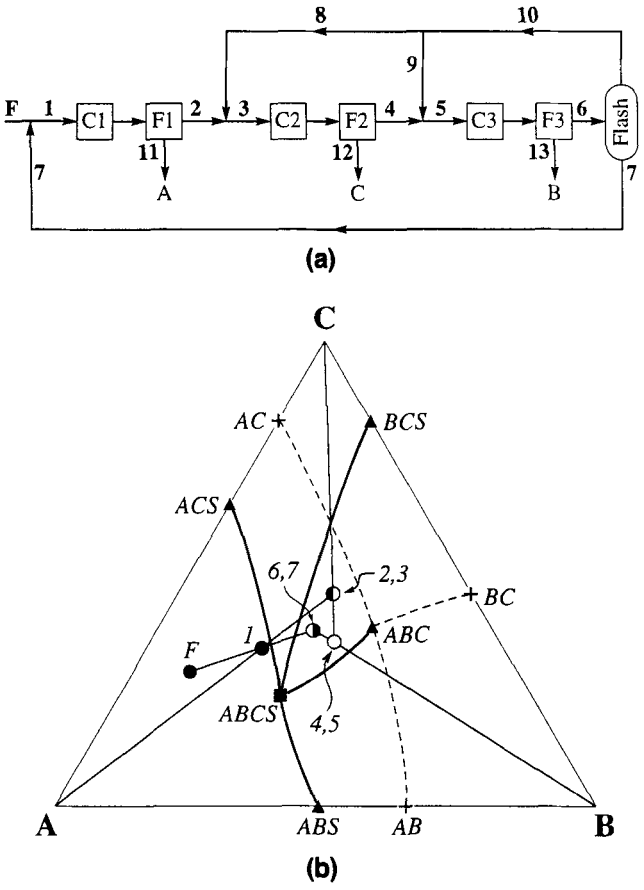


**Figure 8. (*a*) Type IIb process flowsheet; (*b*) type IIb process flowsheet applied to the separation of a system that exhibits PD4 solid-liquid phase behavior.**

Another separation scheme, type IIb, proceeds as shown in Figures 8a and 8b in the separation of solutes exhibiting PD4 phase behavior. Solvent addition is used twice in this separation.

Unlike the first four types described, the last two include stream combination as a means by which to cross a double-saturation surface. Stream combination provides a flexibility that solvent addition and solvent removal do not offer. When solvent addition is applied to a stream, its composition is constrained to move on a straight line toward the 100% solvent composition, denoted by an $S$ in the three-dimensional phase diagrams. When solvent is removed, the composition must move away from $S$. Thus, these two operations can only move a composition directly above or below a surface. On the other hand, when the recycle stream of solutes is combined with another stream in the separation, the resulting composition can lie anywhere on a tie-line between the compositions of the streams being combined. Thus, the new composition can move *closer* to $S$ (as in solvent addition), *farther* from $S$ (as in solvent removal), or *parallel* to the $ABC$ base plane.

Figure 9a is the equipment configuration for type IIIa, which involves stream combination of the recycled solutes as the first operation and then solvent removal as the second. Figure 9b is the Jänecke projection of the PD1 phase diagram and of the type IIIa process compositions. To initiate the type IIIa process, a solvent is added to the feed to create stream 1. Stream 1 is directed to the first crystallizer and filter, where pure $A$ is crystallized and removed. The composition of the stream that emerges from the crystallizer is represented by 2. To move to the next compartment, stream 6 is combined with stream 2. The new stream, 3, has a composition below surface 1 and above surface 2, which puts it in compartment $C$. The subsequent removal of $C$ results in composition 4. In the next step, the evaporator, which is situated between the second and third crystallizers, separates the solutes from the solvent. This ensures that surface 2, which leans away from $C$, is crossed and that compartment $B$ is entered. At this point, it is possible to solidify pure $B$ in the third crystallizer.

It is interesting to note that the type IIIa separation is similar to type Ia (Figures 5a, 5b, and 5c). Both the types Ia and IIIa flowsheets require solvent removal as the second operation and both flowsheets are applicable to the PD1 phase behavior, where surface 1 leans toward $C$. The type IIIa separation crosses surface 1 between streams 2 and 3 by using the solute recycle, stream 6, in a stream combination operation. Although stream 2 contains solvent, stream 6 does not; therefore, the new stream, 3, has proportionally less solvent than does stream 2 and is farther away from $S$ than is stream

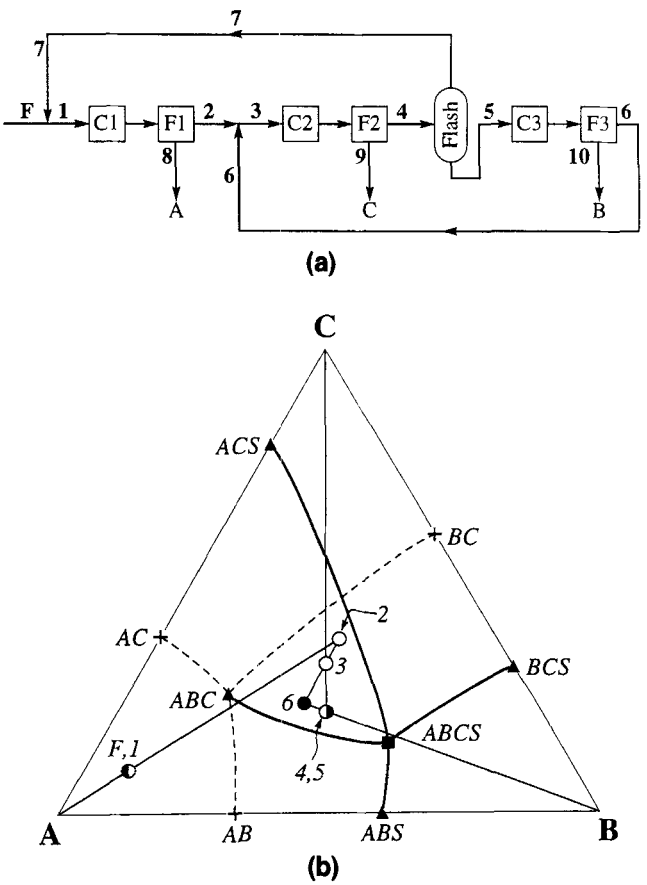


**Figure 9. (*a*) Type IIIa process flowsheet; (*b*) type IIIa process flowsheet applied to the separation of a system showing PD1 solid-liquid phase behavior.**

The type Ia process flowsheet is also applicable.

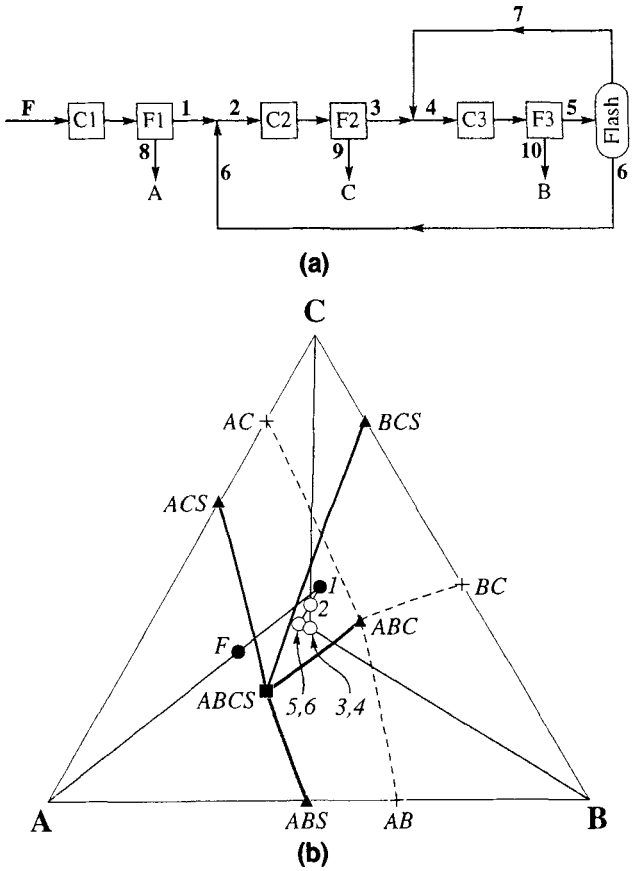


**Figure 10. (a) Type IIIb process flowsheet; (b) type IIIb process flowsheet applied to the separation of a system showing PD4 solid-liquid phase behavior.**

The type IIb process flowsheet is also applicable.

2. In this case, stream combination mimics solvent removal, forcing a composition closer to the *ABC* base and down to the other side of a surface. In effect, type IIIa contains two solvent removal operations, as does type Ia.

The final process configuration is type IIIb (Figure 10a). Figure 10b is a Jänecke projection of the PD4 phase diagram and of the type IIIb process compositions. When the type IIIb flowsheet is applied to the PD4 phase behavior, the stream combination operation is used like solvent addition; surface 1, which leans toward *A*, is crossed as composition 1 becomes composition 2 upon the addition of composition 6. Since the second operation in the type IIIb flowsheet is solvent addition, it is similar to type IIb, a flowsheet requiring two solvent addition operations (Figure 8b).

## Process Sensitivity and Geometric Constraints

The constraints on and sensitivity of an extractive crystallization separation are illustrated by a simulation of the separation of a stream of para-, meta-, and orthoxylene with the solvent butane. The four components are designated by *A*, *B*, *C*, and *S*, respectively. The various input data used in the calculations are summarized in Table 3. Physical constants such as melting temperature, heat of fusion, boiling temperature, and Antoine coefficients can be found in standard references such as the *CRC Handbook of Chemistry and Physics* and *Lange's Handbook of Chemistry*.

Equations 2 and 3 are used to predict approximately the phase behavior of the three solutes and the solvent with the activity coefficient assumed to be close to unity (Figure 11). Since the xylenes and butane exhibit PD1 phase behavior, the type Ia process flowsheet can be used to separate them. The calculational scheme that indicates the location of a process composition relative to the internal surfaces is too complicated to be presented here but can be found elsewhere (Dye, 1994). As discussed previously, the design variables are the composition of the recycle stream ($\boldsymbol{x}(7)$), the ratio of the mole fraction of *B* to the mole fraction of *A* in stream 3 ($R_{BA3}$), and the mole fractions of solvent in streams 3 and 5 [$x_S(3)$ and $x_S(5)$]. With this information, the recycles and all unknown flows and mole fractions are determined by material balances (Eqs. 7–12).

**Table 3. Values of Input Parameters for the Xylenes Plant**

| | | | |
|---|---|---|---|
| *Production rate (kg/yr)* | | | |
| *p*-xylene | | | $53.1\times10^6$ |
| *m*-xylene | | | $31.9\times10^6$ |
| *o*-xylene | | | $21.2\times10^6$ |
| *Feed composition (mole fraction)* | | | |
| *p*-xylene | | | 0.50 |
| *m*-xylene | | | 0.30 |
| *o*-xylene | | | 0.20 |
| *Molecular weight (g/mol)* | | | |
| *p*-, *m*-, *o*-xylene | | | 106.17 |
| *n*-butane | | | 58.12 |
| *Pure component melting temp. (°C)* | | | |
| *p*-xylene | | | 13.2 |
| *m*-xylene | | | −47.8 |
| *o*-xylene | | | −25.2 |
| *n*-butane | | | −138.3 |
| *Heat of fusion (kJ/kmol)* | | | |
| *p*-xylene | | | 16,804 |
| *m*-xylene | | | 11,554 |
| *o*-xylene | | | 13,611 |
| *n*-butane | | | 4,664 |
| *Eutectic temp. (°C)* | | | |
| Binary | | | |
| *p*-xylene and *m*-xylene | | | −52.5 |
| *p*-xylene and *o*-xylene | | | −35.1 |
| *m*-xylene and *o*-xylene | | | −61.3 |
| *p*-xylene and *n*-butane | | | −138.3 |
| *m*-xylene and *n*-butane | | | −138.8 |
| *o*-xylene and *n*-butane | | | −138.4 |
| Ternary | | | |
| *p*-xylene, *m*-xylene, and *o*-xylene | | | −63.7 |
| *p*-xylene, *m*-xylene, and *n*-butane | | | −138.8 |
| *p*-xylene, *o*-xylene, and *n*-butane | | | −138.4 |
| *m*-xylene, *o*-xylene, and *n*-butane | | | −138.9 |
| Quaternary | | | |
| *p*-xylene, *m*-xylene, *o*-xylene, and *n*-butane | | | −138.9 |
| *Antoine coefficients* | | | |
| | A | B | C |
| *p*-xylene | 6.99052 | 1,453.430 | 215.31 |
| *m*-xylene | 7.00908 | 1,462.266 | 215.11 |
| *o*-xylene | 6.99891 | 1,474.679 | 213.69 |
| *n*-butane | 6.80896 | 935.86 | 238.73 |
| *Boiling temp. at 1 atm (°C)* | | | |
| *p*-xylene | | | 138.35 |
| *m*-xylene | | | 139.10 |
| *o*-xylene | | | 144.42 |
| *n*-butane | | | −0.6 |

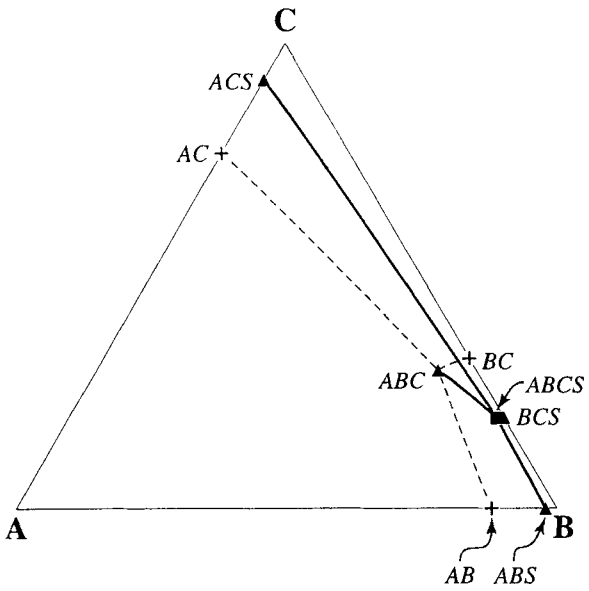


**Figure 11. Solid-liquid-phase diagram for xylenes and butane.**

To ascertain the effect of each design variable on the separation, the relative sizes of the recycle streams are examined, using the feed as a basis of comparison. The following three ratios are considered: $R_{STF}$, $R_{S9F}$, and $R_{ABCF}$. These are the ratio of total recycled solvent flow to feed flow, ratio of recycled solvent flow from the second column (stream 9) to feed flow, and ratio of total recycled solutes flow to feed flow, respectively:

$$R_{STF} = \frac{F_S(10)}{F_{AF} + F_{BF} + F_{CF}} \tag{14}$$

$$R_{S9F} = \frac{F_S(9)}{F_{AF} + F_{BF} + F_{CF}} \tag{15}$$

$$R_{ABCF} = \frac{F_A(7) + F_B(7) + F_C(7)}{F_{AF} + F_{BF} + F_{CF}}. \tag{16}$$

A base case is chosen with the following feed composition: $F_{AF} = 500.0 \times 10^3$ kmol/yr, $F_{BF} = 300.0 \times 10^3$ kmol/yr, $F_{CF} = 200.0 \times 10^3$ kmol/yr, and $F_{SF} = 0.0$ kmol/yr. The base case values of the design variables are $x_S(3) = 0.78$; $x_S(5) = 0.50$; $x_A(7) = 0.063$; $x_B(7) = 0.636$; and $R_{BA3} = 11.2$. As will be seen below, these values are close to a local minimum in terms of recycle flows. While the other design variables are held constant, each of the four design variables is varied one at a time.

### *Effect of changes in $x_S(3)$*

Figure 12 demonstrates the effect of changes in $x_S(3)$. As the mole fraction $x_S(3)$ is lowered from 0.96 to 0.78, $R_{STF}$ decreases dramatically. This result is expected since the ratio $x_S(3)/x_B(3)$ in Eq. 12 decreases nonlinearly with decreases in $x_S(3)$. As $x_S(3)$ is lowered, composition 3 moves closer to the base of the tetrahedral phase diagram, and the amount of recycled solvent moves toward zero. The value of $x_S(3)$, however, is subject to the thermodynamic constraint that composition 3 be located in compartment $A$, above surface 1 (Figure 5b). In the case of xylenes, cocrystallization would occur at an $x_S(3)$ of 0.78 or less, as indicated in Figure 12. In other words, $x_S(3)$ should be as low as possible in order to minimize the size of the total solvent recycle stream, but should not be so low that the product is impure. Since $x_S(3)$ does not appear in the material balance for solvent recycle from the second evaporator (Eq. 10), $R_{S9F}$ remains unchanged by the variation in $x_S(3)$. The same can be said of $R_{ABCF}$ because $x_S(3)$ is not part of any of the solute balances (Eqs. 7–9).

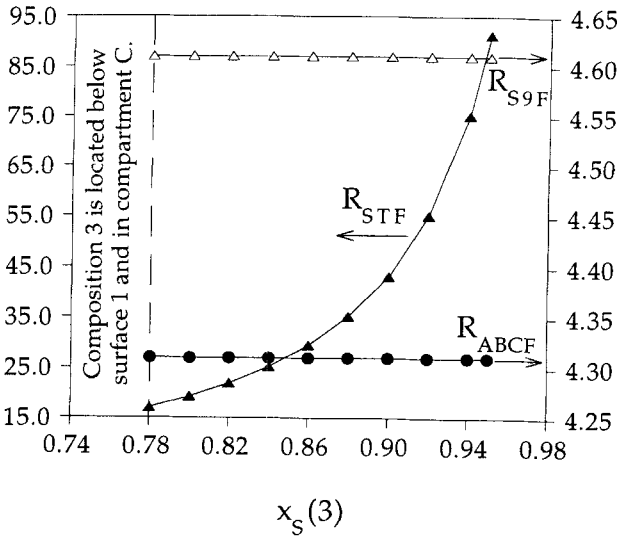


**Figure 12. Effect of changes in $x_S(3)$.**

### *Effect of changes in $x_S(5)$*

The results of changes in $x_S(5)$ are reported in Figure 13. The parameter $x_S(5)$ is not part of the solute recycle bal-

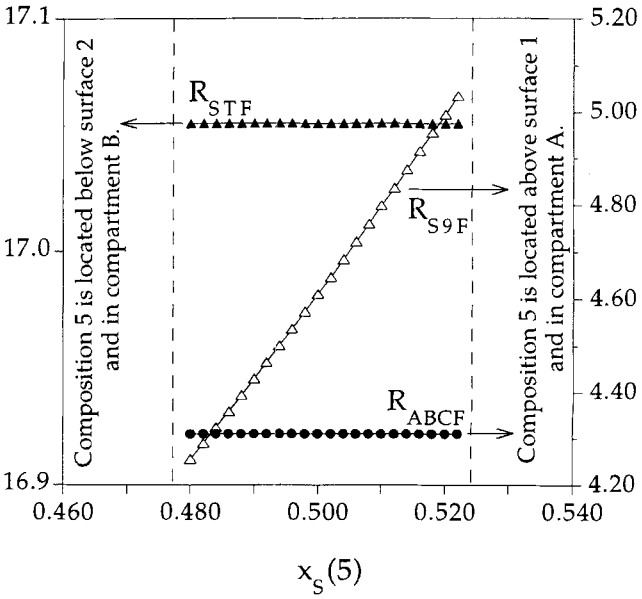


**Figure 13. Effect of changes in $x_S(5)$.**

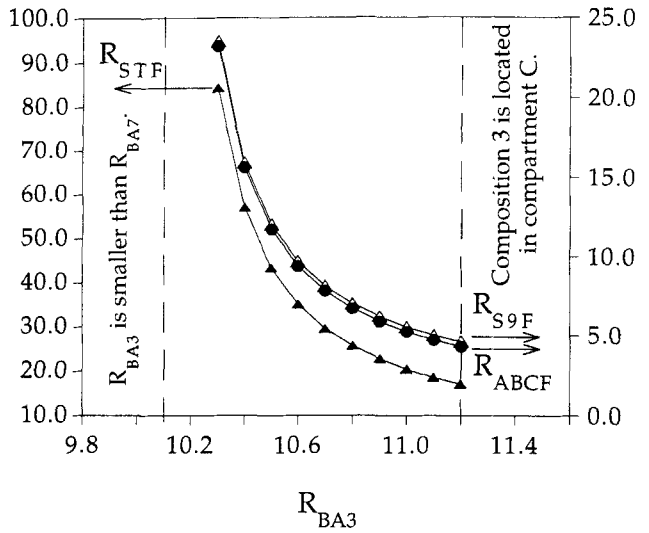


**Figure 14. Effect of changes in $R_{BA3}$.**

ances; thus, $R_{ABCF}$ is a horizontal line. $R_{STF}$ is also horizontal because $x_S(5)$ does not determine the overall solvent flow (Eq. 12). When $x_S(5)$ is decreased, the flow rate of stream 9 decreases (Eq. 10) and that of stream 8 increases (Eq. 11), leaving stream 10 unchanged. In fact, $x_S(5)$ only affects the distribution of the total solvent recycle between streams 8 and 9. Figure 13 indicates that $x_S(5)$ should be as far below surface 1 as possible in order to minimize the amount of solvent evaporated in the second flash operation, but a review of Figure 5c reveals that composition 5 must also be above surface 2 in order to be located in compartment *B*. This feasible region between surfaces 1 and 2 is marked on Figure 13.

### *Effect of changes in the ratio $R_{BA3}$*

$R_{BA3}$ figures prominently in the material balances and an increase in $R_{BA3}$ causes a decrease in $R_{ABCF}$, $R_{STF}$, and $R_{S9F}$ (Figure 14). As $R_{BA3}$ is increased, the projection of composition 3 moves toward the *BC* edge of the phase diagram (Figure 5b). Thus, increases in $R_{BA3}$ are constrained by the fact that the projection of composition 3 must remain on the projection of surface 1—in other words, in compartment *A*. Decreases in $R_{BA3}$ are limited by the fact that it cannot be less than $R_{BA7}$, a fixed design variable. Both the upper and lower limit on $R_{BA3}$ are indicated in Figure 14.

### *Effect of changes in the recycle composition*

If the composition of the solute recycle is changed, there is a significant effect on the magnitudes of the solute and solvent recycles. First, $x_A(7)$ is altered slightly from its base case value of 0.063 to a new value, 0.062, while keeping $x_B(7)$ at the base case value. As can be seen in the second row of Table 4, all three recycles ($R_{ABCF}$, $R_{STF}$, $R_{S9F}$) increase as compared to the base case. Then, $x_B(7)$ is increased from its base case value of 0.636 to 0.638, while keeping $x_A(7)$ at the base case value. Again, all three recycle ratios increase from their base case values. Note that the projection of composition 7 should be kept within the triangle formed by the overlap between surfaces 1 and 2 (Figure 5b).

**Table 4. Effect of Changes in Recycle Composition**

| | $R_{STF}$ | $R_{S9F}$ | $R_{ABCF}$ |
|---|---|---|---|
| Base case | 17.1 | 4.61 | 4.31 |
| $x_A(7) = 0.062$ | 20.0 | 5.44 | 5.14 |
| $x_B(7) = 0.638$ | 17.5 | 4.74 | 4.44 |

## Optimal Characteristics of Phase Diagram and Solvent Selection

The solvent to be used in the type Ia separation should create phase behavior with characteristics that accommodate the optimum values of the design variables as outlined previously. First, the triple-saturation trough connecting *ACS* to *ABCS* should be close to the *BC* edge of the phase diagram (Figure 5b). This would allow the tie-line connecting *C* and process composition 3 to swing to the right. This implies an increase in the value of $R_{BA3}$ and a significant reduction in all the flows (Figure 14). Second, all of surfaces 1 and 2 should be close to the base of the tetradedral diagram. This would allow $x_S(3)$ to be small, thus minimizing the total recycled solvent flow. However, this implies that the solvent has relatively high melting and boiling points compared to those of the solutes. Thus, the disadvantage of having surfaces 1 and 2 close to the base is that larger distillation columns are required to separate a higher-boiling solvent from the solutes in all six equipment configurations. Finally, the size and orientation of surfaces 1 and 2 should be such that compositions 4 and 5, and compositions 6 and 7, can be quite separated; this condition allows a maximum amount of solute to be removed in each pass, minimizing solute recycle.

## Capital and Operating Costs for Extractive Crystallization

The separation of a system with nonideal liquid-phase behavior and with properties typical of organic systems is used to assess the cost of an extractive crystallization separation (Table 5). The liquid-phase activity coefficient $\gamma$ is calculated with the two-suffix Margules equation (Malesinski, 1965):

$$RT \ln \gamma_k = \frac{1}{2} \sum_{i=1}^{c} \sum_{j=1}^{c} (A_{i,k} + A_{j,k} - A_{i,j}) x_i x_j. \quad (17)$$

The $A_{i,j}$ quantify the interaction between pairs of components with $A_{i,j} = A_{j,i}$ and $A_{i,i} = 0$.

Figure 15a is a plot of the solid-liquid tetrahedral phase diagram and Figure 15b is a plot of the corresponding Jänecke projection. Note the slight curvature of the double- and triple-saturation troughs, a feature that does not exist when the liquid phase is ideal. This tends to cause the surfaces in the projected phase diagram to be larger than they would be were there no nonidealities.

Figure 15b reveals that this system can be separated by the type Ia process configuration. The values of the design variables and corresponding recycle ratios are listed in Table 6. Based on these parameters, the flow rates and compositions of all streams in the separation are determined, the equipment sizes are estimated, and the eight most significant annual equipment and operating expenses are calculated. The

**Table 5. Values of Input Parameters for the Separation of the Nonideal System**

| | | | |
|---|---|---|---|
| *Production rate (kg/yr)* | | | |
| *A* | | | $66.15\times10^5$ |
| *B* | | | $14.70\times10^5$ |
| *C* | | | $66.15\times10^5$ |
| *Feed composition (mole fraction)* | | | |
| *A* | | | 0.45 |
| *B* | | | 0.10 |
| *C* | | | 0.45 |
| *Molecular weight (g/mol)* | | | |
| *A, B, C* | | | 147.0 |
| *S* | | | 58.0 |
| *Pure component melting temp. (°C)* | | | |
| *A* | | | 75.88 |
| *B* | | | 59.65 |
| *C* | | | 44.19 |
| *S* | | | −43.15 |
| *Heat of fusion (kJ/kmol)* | | | |
| *A* | | | 17,153 |
| *B* | | | 12,639 |
| *C* | | | 12,928 |
| *S* | | | 9,607 |
| *Eutectic temp. (°C)* | | | |
| Binary | | | |
| *A* and *B* | | | 22.42 |
| *A* and *C* | | | 15.75 |
| *B* and *C* | | | 3.44 |
| *A* and *S* | | | −46.58 |
| *B* and *S* | | | −52.28 |
| *C* and *S* | | | −52.70 |
| Ternary | | | |
| *A, B,* and *C* | | | −7.65 |
| *A, B,* and *S* | | | −54.31 |
| *A, C,* and *S* | | | −54.70 |
| *B, C,* and *S* | | | −58.82 |
| Quaternary | | | |
| *A, B, C,* and *S* | | | −60.20 |
| *Antoine coefficients* | | | |
| | A | B | C |
| *A* | 6.99052 | 1,453.430 | 175.31 |
| *B* | 7.00908 | 1,462.266 | 175.11 |
| *C* | 6.99891 | 1,474.679 | 173.69 |
| *S* | 6.80896 | 935.86 | 238.73 |
| *Boiling temperature at 1 atm (°C)* | | | |
| *A* | | | 208.35 |
| *B* | | | 209.10 |
| *C* | | | 214.41 |
| *S* | | | −2.05 |
| *Interaction parameter (cal/mol)* | | | |
| $A_{A,S}$ | | | −230.0 |
| $A_{B,S}$ | | | −280.0 |
| $A_{C,S}$ | | | −230.0 |
| $A_{A,B}$ | | | −200.0 |
| $A_{A,C}$ | | | −200.0 |
| $A_{B,C}$ | | | −230.0 |

annual equipment costs are obtained by applying a capital charge factor of 1/3 to the capital costs. Details of the equipment and cost models are reported elsewhere (Dye, 1995). The equipment costs are for the refrigerant compressors, refrigerant condensers and evaporators, crystallizer tanks, filters, and solvent evaporators. Operating costs are composed of the cost of electricity for the refrigerant compressors, steam for the solvent evaporators, and cooling water for the refrigerant condensers. The relative contribution of each of the eight major categories to the total annualized cost of $2.76

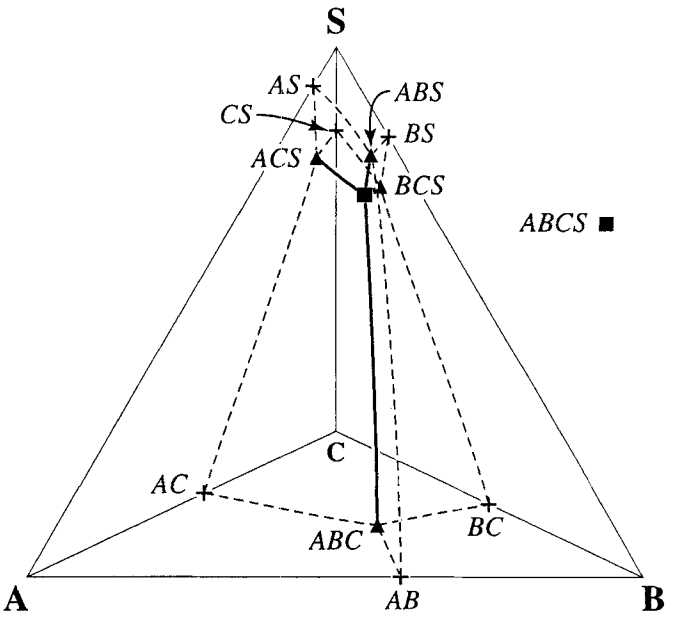


(a)

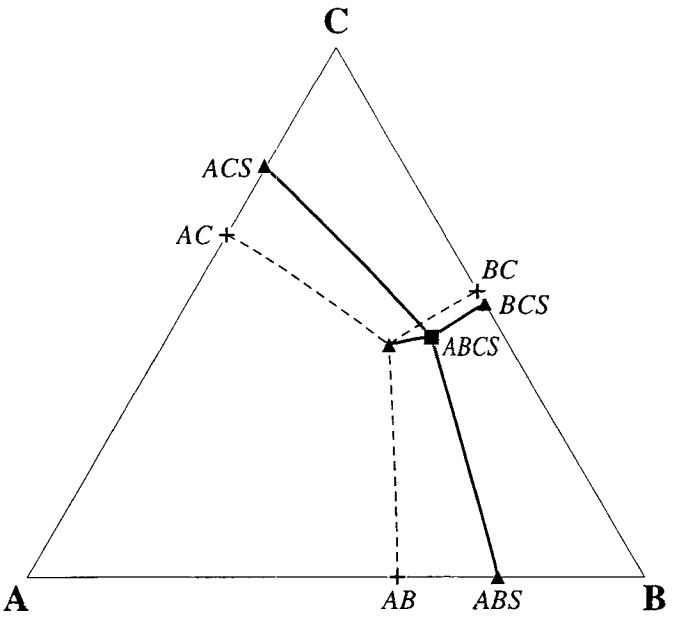


(b)

**Figure 15. (*a*) Solid-liquid tetrahedral phase diagram for a nonideal system; (*b*) Jänecke projection for the nonideal system.**

**Table 6. Design Variables and Recycle Ratios for the Separation of the Nonideal System**

| | |
|---|---|
| *Design variables (mole fraction)* | |
| $R_{BA3}$ | 2.28 |
| $x_S(3)$ | 0.48 |
| $x_S(5)$ | 0.28 |
| $x_A(7)$ | 0.17 |
| $x_B(7)$ | 0.38 |
| *Recycle ratios (molar ratios)* | |
| $R_{ABCF}$ | 13.16 |
| $R_{S9F}$ | 5.16 |
| $R_{STF}$ | 12.65 |

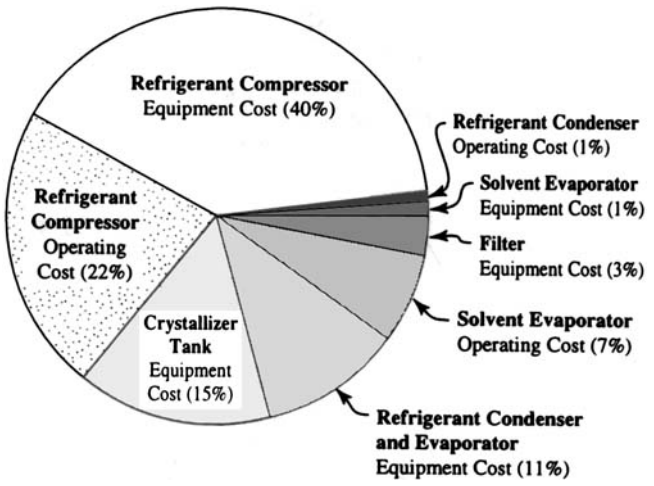


**Figure 16. Annualized equipment costs and operating costs as a percentage of the total cost.**

million (1994 dollars) is pictured in Figure 16. Not surprisingly, the largest contribution to the total cost comes from the refrigerant compressors.

The vessel costs and some of the heating/cooling costs for this separation would decrease with a decrease in recycle flow rates, and the lowest recycle flow rates occur when the design variables are chosen such that the process compositions are as close to the eutectics as possible without bringing about coprecipitation. Since the eutectics are the coldest locations on the phase diagram, the conditions that would require the lowest recycle would demand the most extensive refrigeration. Hence, there is a tradeoff between the recycle sizes and refrigeration requirements.

It is likely that a cost even lower than \$2.76 million could be found for this separation by searching a range of design variables to determine the conditions where the tradeoff between the recycle flow rates and the refrigeration requirements gives a minimum cost. Although no attempt is made to search for such a minimum, it is clear that, for the average organic system, extractive crystallization can be an attractive separation method.

## Two-Loop Separations

For some systems, a two-loop extractive crystallization separation may prove more desirable than a one-loop separation. For example, a two-loop separation is shown in Figure 17a. Note that the phase diagram is not exactly PD5 in that surface 1 is twisted (Figure 17b). In this case, $A$ can be removed as usual. It is inconvenient, however, to cross into compartment $C$ by means of solvent removal because surface 1 is rather narrow as viewed through $S$. An alternative is to direct the effluent from the first crystallizer, stream 2, to the second crystallizer, where it is cooled and filtered until composition 3 is reached. Since the process compositions follow the $AC$ binary eutectic trough, cocrystallization occurs. Assuming that $A$, $C$, and another solvent $S'$ exhibit type I phase behavior as defined in Rajagopal et al. (1991), we can completely separate $A$ and $C$ using the equipment configuration shown in the second loop of Figure 17a. Then, the addition of solvent to stream 3 places stream 4 in compartment $B$, where pure $B$ is recovered. Stream 5, the effluent mother liquor from crystallizer $C3$, is sent to a flash unit to separate the solvent from the solutes for recycle.

Another two-loop separation is shown in Figures 18a and 18b. In its initial stages, this separation resembles type Ib. Surface 1 leans away from $A$, and therefore solvent removal is used to cross this surface after an amount of $A$ equal to that in the feed has been removed from stream 2. Stream 4, whose composition is in compartment $C$, is directed to crystallizer 2 in order to recover some $C$. It is at this point that this separation differs from type Ib; solvent addition cannot be used to cross surface 2. Instead, stream 5 is cooled to obtain a mixture of crystals of $B$ and $C$, which are sent to a binary separation process. Assuming that $A$, $C$, and another solvent $S'$ exhibit type II phase behavior as defined in Rajagopal et al. (1991), we can completely separate $A$ and $C$ using the equipment configuration shown in Figure 18a. Stream 6, the effluent from crystallizer 3, is recycled to mix with the feed stream.

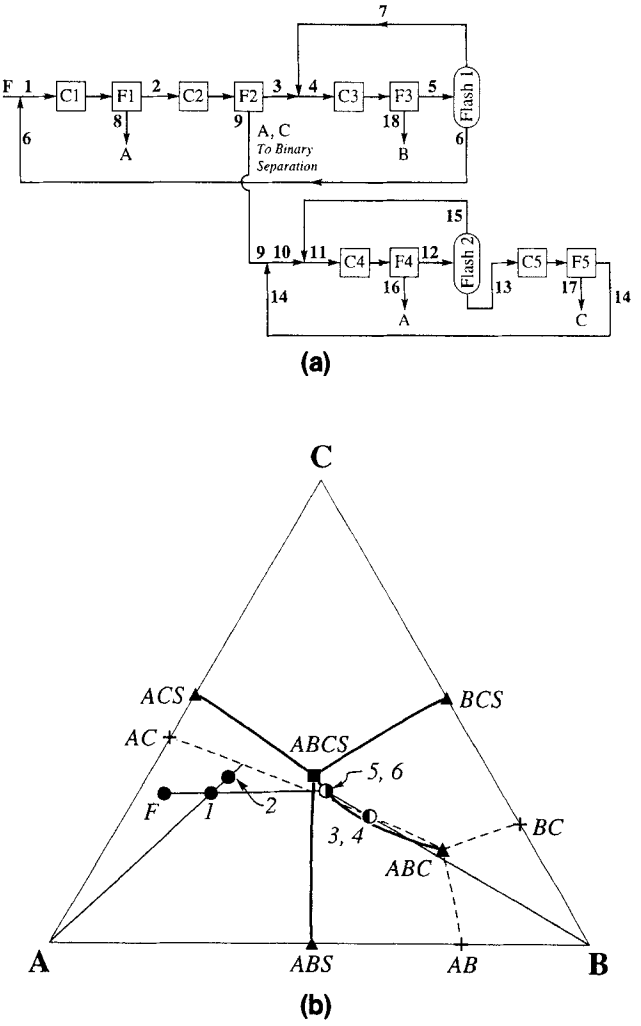


**Figure 17. (a) Two-loop process flowsheet; (b) phase diagram and process paths for the two-loop separation.**

Type I separation is assumed for the second loop.

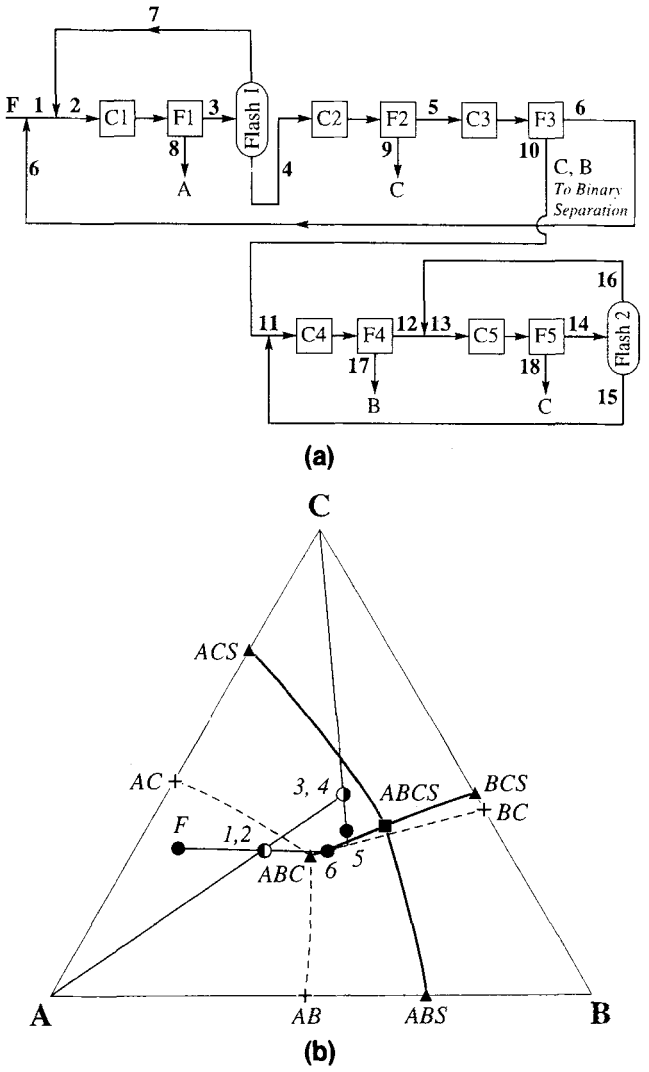


**Figure 18. (*a*) Another two-loop process flowsheet; (*b*) phase diagram and process paths for the two-loop separation.**

Type II separation is assumed for the second loop.

## Conclusions

Eutectics prevent the complete separation of a multicomponent mixture by simple crystallization. With the use of an extraneous solvent, extractive crystallization offers a way to bypass these thermodynamic barriers. The combination of three operations—stream combination, solvent removal, and solvent addition—results in six flowsheet structures that can be applied to any of six general phase behaviors for a four-component system. Although the phase diagrams considered are simple-eutectic systems, the design methodology is applicable to mixtures containing multiple eutectics and compound formation, as demonstrated in Rajagopal et al. (1991) for a three-component system. The capability of the extractive crystallization technique to bypass eutectic barriers also allows the avoidance of those complicated regions in the phase diagram.

To facilitate process synthesis, design equations, a process sensitivity analysis, and a cost analysis are provided. Based on the sensitivity analysis of the separation of para-, meta-, and ortho-xylene, those features of a phase diagram favorable to the use of extractive crystallization are identified; however, no attempt is made to characterize the solvent that would create those features. It is highly desirable to predict the molecular structure of a solvent or those of a combination of solvents for a given mixture of three solutes. Efforts in the use of computational chemistry in process synthesis might well provide an answer to this question (Mavrovouniotis, 1990). The extractive crystallization separation of the xylene mixture is clearly not economical because of the very low temperature of the quaternary eutectic and ternary eutectics. The cost analysis is based on a hypothetical system similar to mixtures such as the dichlorobenzenes. As expected, refrigeration is the major cost. However, refrigeration is not always required in extractive crystallization. Consider a mixture of para-, meta- and orthonitrophenol, which have melting points of 114, 97, and 45°C, respectively, and a ternary eutectic temperature of 21.5°C. Depending on the physical characteristics of the solvent used for a separation of the nitrophenols, the quaternary eutectic temperature of this system could be much higher than that of the xylenes. Since this technique is intended for species with high boiling and melting points, extractive crystallization should be even more competitive.

Solid-liquid phase behavior is predicted using the general solubility equation. The solid phase is assumed to be a pure component or a mixture of pure components. If the liquid phase is nonideal, the general two-suffix Margules equation is used to calculate the activity coefficients. In contrast to the abundance of data for vapor-liquid equilibria, woefully little exists for solid-liquid systems. We recommend that phase behavior be determined experimentally (for example, Ozawa and Matsuoka, 1989), focusing on regions of the phase diagram at which the process flows are most sensitive to changes in design variables.

A number of extensions of this extractive crystallization work are desirable. First, the material balance equations are based on two simplifying assumptions: there is no loss of solute in the mother liquor trapped in the filter cakes, and the solvent can be completely separated from the solutes in a flash unit or a distillation column. While these equations are adequate for conceptual design, more detailed balances should be developed. Second, impurities are often present in commercial processes. For this reason, an exit point should be included in the flowsheet configurations. Third, extractive crystallization should be considered in relation to other existing crystallization-based separation schemes (Dye et al., 1995) as well as to all other separation techniques. The final and obvious extension is a design methodology for the use of extractive crystallization for a mixture with four or more solutes. This is an interesting problem in that the phase behavior and the process paths can no longer be viewed graphically. However, as previously mentioned, it is more likely that extractive crystallization would be used in conjunction with other separation techniques for a higher *multidimensional* system.

## Acknowledgment

We express our appreciation to the National Science Foundation, grant no. CTS-9220196, for support of this research. We would also like to thank Ms. Pamela Stephan for her graphic artwork.

## Notation

$c$ = total number of components
$F_{iF}$ = feed flow rate of component $i$ (mol/yr)
$F_i(j)$ = flow rate of component $i$ in stream $j$ (mol/yr)
$R$ = ideal gas constant (cal/mol·K)
$R_{BA7}$ = ratio of mole fraction $B$ to mole fraction $A$ in stream 7
$R_{SB3}$ = ratio of mole fraction $S$ to mole fraction $B$ in stream 3
$x_i(j)$ = liquid mole fraction of component $i$ in stream $j$

## Literature Cited


Barnicki, S. D., and J. R. Fair, "Separation System Synthesis: A Knowledge-Based Approach: 1. Liquid Mixture Separations," *Ind. Eng. Chem. Res.*, **29**, 421 (1990).

Chivate, M. R., and S. M. Shah, "Separation of *m*-Cresol and *p*-Cresol by Extractive Crystallization," *Chem. Eng. Sci.*, **5**, 232 (1956).

Dale, G. H., "Crystallization, Extractive and Adductive," *Encycl. Chem. Process. Des.*, **13**, 456 (1981).

Dikshit, R. C., and M. R. Chivate, "Separation of Ortho and Para Nitrochlorobenzenes by Extractive Crystallization," *Chem. Eng. Sci.*, **25**, 311 (1970).

Douglas, J. M., *Conceptual Design of Chemical Processes*, McGraw-Hill, New York (1988).

Douglas, P. L., M. K. Garg, J. G. Linders, and S. K. Mallick, "A New Algorithm for Selection of Separation Technologies," *Trans. Inst. Chem. Eng.*, Part A, **71**, 479 (1993).

Dye, S. R., PhD Diss., Dept. of Chemical Engineering, Univ. of Massachusetts, Amherst, MA (1995).

Dye, S. R., D. A. Berry, and K. M. Ng, "Synthesis of Crystallization-Based Separation Schemes," *Proc. Found. Comput.-Aided Proc. Des.*, in press (1995).

Findlay, R. A., and J. A. Weedman, "Separation and Purification by Crystallization," *Advances in Petroleum Chemistry and Refining*, Vol. I, K. A. Kobe and J. A. McKetta, eds., Interscience, New York, p. 119 (1958).

Gilbert, S. W., "Melt Crystallization: Process Analysis and Optimization," *AIChE J.*, **37**, 1205 (1991).

Haase, R., and H. Schönert, *Solid-Liquid Equilibrium*, Pergamon, New York (1969).

Malesinski, W., *Azeotropy and Other Theoretical Problems of Vapour-Liquid Equilibrium*, Interscience, New York (1965).

Matsuoka, M., "Solid-Liquid Phase Equilibria of Organic Mixtures," *Bunri Gijutsu*, **6**, 245 (1977).

Mavrovouniotis, M. L., "Estimation of Properties from Conjugate Forms of Molecular Structures: The ABC Approach," *Ind. Eng. Chem. Res.*, **29**, 1943 (1990).

Nagahama, K., D. Hoshino, K. Maeda, and M. Itoh, "Vapor-Liquid-Solid Equilibria of Ternary, Liquefied Gas-Benzene-Cyclohexane Systems and Their Application in a New Process of Crystallization," *Int. Chem. Eng.*, **31**, 359 (1991).

Ozawa, R., and M. Matsuoka, "Determination of Solid-Liquid Phase Equilibrium of Organic Ternary Eutectic Mixtures by Differential Scanning Calorimeter—The *o*-, *m*-, and *p*-nitroaniline System," *J. Crystal Growth*, **98**, 411 (1989).

Paul, E. L., and C. B. Rosas, "Challenges for Chemical Engineers in the Pharmaceutical Industry," *Chem. Eng. Prog.*, **86**(12), 17 (1990).

Rajagopal, S., K. M. Ng, and J. M. Douglas, "Design and Economic Trade-Offs of Extractive Crystallization Processes," *AIChE J.*, **37**, 437 (1991).

Rajagopal, S., K. M. Ng, and J. M. Douglas, "A Hierarchical Procedure for the Conceptual Design of Solids Processes," *Comput. Chem. Eng.*, **16**, 675 (1992).

Ricci, J. E., *The Phase Rule and Heterogeneous Equilibrium*, Van Nostrand, New York (1951).

Sciance, C. T., and L. S. Scott, "Process for Separation of Glutaric, Succinic and Adipic Acids," U.S. Patent 3,338,959 (1967).

Slaughter, D. W., and M. F. Doherty, "Calculation of Solid-Liquid Equilibrium and Crystallization Paths for Melt Crystallization Processes," *Chem. Eng. Sci.*, in press (1995).

Tare, J. P., and M. R. Chivate, "Separation of Close Boiling Isomers by Adductive and Extractive Crystallization," *AIChE Symp. Ser.*, **72**(153), 95 (1976).

Walas, S. M., *Phase Equilibria in Chemical Engineering*, Butterworth, Boston (1985).

Westerberg, A. W., "Process Synthesis: A Morphological View," in *Recent Developments in Chemical Process and Plant Design*, Y. A. Liu, H. A. McGee, Jr., and W. R. Epperly, eds., Wiley, New York (1987).


*Manuscript received May 31, 1994, and revision received Aug. 11, 1994.*